

UC Santa Barbara

UC Santa Barbara Previously Published Works

Title

Optimization of the surface and structural quality of N-face InN grown by molecular beam epitaxy

Permalink

<https://escholarship.org/uc/item/968441jh>

Journal

Applied Physics Letters, 89(7)

ISSN

0003-6951

Authors

Koblmuller, G
Gallinat, C S
Bernardis, S
[et al.](#)

Publication Date

2006-08-01

Peer reviewed

Optimization of the surface and structural quality of N-face InN grown by molecular beam epitaxy

G. Koblmüller,^{a)} C. S. Gallinat, S. Bernardis, and J. S. Speck
Materials Department, University of California, Santa Barbara, California 93106-5050

G. D. Chern, E. D. Readinger, H. Shen, and M. Wraback
U.S. Army Research Laboratory, Sensors and Electron Devices Directorate, 2800 Powder Mill Road,
Adelphi, Maryland 20783

(Received 29 March 2006; accepted 26 June 2006; published online 14 August 2006)

The authors demonstrate the impact of growth kinetics on the surface and structural properties of N-face InN grown by molecular beam epitaxy. Superior surface morphology with step-flow growth features is achieved consistently under In-rich conditions in a low-temperature region of 500–540 °C. Remarkably, off-axis x-ray rocking curve (ω scans) widths are found to be independent of the growth conditions. The band gap determined from optical absorption measurements of optimized InN is 0.651 eV, while photoluminescence peak emission occurs at even lower energies of ~ 0.626 eV. Hall measurements show room temperature peak electron mobilities as high as $2370 \text{ cm}^2/\text{V s}$ at a carrier concentration in the low 10^{17} cm^{-3} region. Analysis of the thickness dependence of the carrier concentration demonstrates a *n*-type surface accumulation layer with a sheet carrier concentration of $\sim 3 \times 10^{13} \text{ cm}^{-2}$. © 2006 American Institute of Physics. [DOI: 10.1063/1.2335685]

Over the past few years, InN has fueled tremendous interest because the fundamental band gap energy has been revised to approximately 0.7 eV.^{1–3} Consequently, InN is becoming increasingly attractive not only as a near-infrared (IR) material for optoelectronic applications, including its possible performance as a terahertz emitter,⁴ but also for extending the emission of light emitting diodes from deep ultraviolet to near IR, if alloyed with GaN or AlN.⁵ Beyond this, superior electronic transport properties, i.e., high electron peak velocities⁶ and mobilities, are expected due to its small electron effective mass of $\approx 0.04m_0$.^{6,7} Indeed, a few experimental studies of undoped InN point to room temperature electron mobilities exceeding $2000 \text{ cm}^2/\text{V s}$.^{8,9}

For the In-face orientation, numerous attempts, using mainly plasma-assisted molecular beam epitaxy (MBE), have been undertaken to generate good crystal and surface quality for improved optical and transport properties. The implementation of various buffer layers, such as AlN,¹⁰ low-temperature InN,¹¹ and GaN,^{9,12} has helped especially to reduce free electron carrier concentration and sharpen the optical absorption edge, partly overcoming the lack of a near-lattice-matched substrate. However, the low InN decomposition temperature presents significant growth challenges, limiting the growth temperature to ≈ 500 °C.^{13,14}

Most recently, the challenges of InN deposition have been addressed by growing films along the thermally more stable N-face orientation,^{15,16} where growth temperatures up to 600 °C seem feasible. Higher structural quality InN films with sharp step-flow surface features may be achieved, even under N-rich growth conditions. This appears contradictory to the established knowledge of high adatom diffusion under purely metal-rich conditions, as in GaN (Ref. 17) or AlN (Ref. 18) growth. In this letter, we investigate these important aspects of N-face InN growth, with special emphasis on

the effect of growth kinetics on the advancement of the physical properties.

As substrates for N-face growth, we used high-quality freestanding N-face GaN templates provided by Lumilog with threading dislocation densities specified to be less than $1 \times 10^8 \text{ cm}^{-2}$. To produce a surface free of contamination and of good interface quality we have grown an ≈ 40 nm thick GaN buffer layer under Ga-rich conditions at a temperature of 700 °C. Both the GaN buffer and InN layer growths were performed in an Epi 620 MBE system using standard effusion cells for Ga and In, and an Epi Unibulb radio frequency plasma source for supplying active nitrogen. A pyrometer was used to measure the substrate temperature *in situ*. We give all molecular fluxes in terms of potential growth rate in units of nm/min, as calibrated from thickness measurements of InN films grown under In-rich and N-rich conditions at temperatures for which thermal decomposition was negligible. High-resolution x-ray rocking curves (ω scans) and ω - 2θ scans were performed using a triple-axis diffractometer with a resolution limit of ~ 10 arc sec. The structural quality of the InN films was correlated with the surface morphology by employing atomic force microscopy (AFM). In addition, we have selected optimized InN films on N-face GaN layers (200 nm thick) grown on NOVASiC polished C-face 6H-SiC substrates^{19,20} for optical spectroscopy, using a combination of photoluminescence (PL) and optical absorption obtained from reflectance and transmission measurements. To identify transport properties, we performed Hall measurements in the van der Pauw geometry on as-grown InN layers on the buffered, semi-insulating C-face 6H-SiC substrates.

Reflection high energy electron diffraction (RHEED) was used to confirm the N-face growth direction prior to each InN growth. By cooling the GaN buffer layer to temperatures below ~ 620 °C we observed a distinct 3×3 RHEED reconstruction, which is a well known characteristic of a N-face GaN growth surface.²¹ The N-face InN layers presented here were grown at different temperatures and

^{a)}Electronic mail: gregor@engineering.ucsb.edu

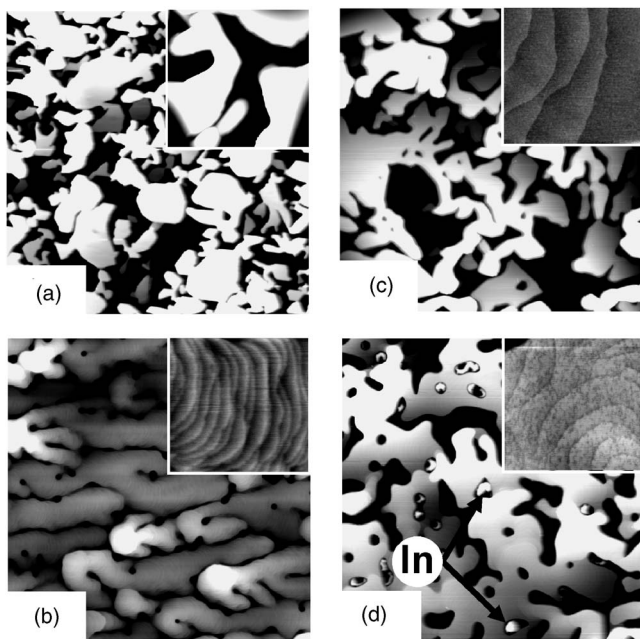


FIG. 1. AFM micrographs [$10 \times 10 \mu\text{m}^2$ and $1 \times 1 \mu\text{m}^2$ (insets)] of InN layers grown on freestanding GaN; growth temperatures and In/N flux ratios are (a) 530 °C and 0.9, (b) 530 °C and 1.4, (c) 595 °C and 0.9, and (d) 595 °C and 1.4. The height scale of the inset images is 2 nm for all samples, but for the larger images it is 50 nm for (a) and (c) and 20 nm for (b) and (d).

In/N flux ratios. To achieve different flux ratios, we kept the N flux constant at 7.5 nm/min and varied only the In flux, from N-rich (In/N=0.9) to In-rich droplet conditions (In/N=1.4). The designation of these growth regimes and their intricate relationship with thermal decomposition have been elaborated in detail and will be published elsewhere.²² In Fig. 1, typical AFM surface morphologies are shown for nominally $\sim 0.9 \mu\text{m}$ thick InN layers grown at two temperatures (530 and 595 °C) and In/N ratios of 0.9 and 1.4, respectively. The measured InN thicknesses from cross-sectional scanning electron microscopy coincided with the nominal thickness for layers grown at 530 °C ($\sim 0.87 \mu\text{m}$), but were slightly reduced due to thermal decomposition for layers grown at 595 °C ($\sim 0.67 \mu\text{m}$). InN layers grown under N-rich growth conditions exhibit the roughest surfaces with root-mean-square (rms) values of 54.1 nm [Fig. 1(a)] and 29.6 nm [Fig. 1(c)] over a $10 \times 10 \mu\text{m}^2$ area. In contrast, when the growth was performed under In-rich droplet conditions and low temperature ($T=530$ °C) significantly improved surface quality was achieved (rms roughness = 6.6 nm) [Fig. 1(b)]. Imaging the areas in between the few and randomly distributed In droplets displays large atomically flat terraces with clear step-flow growth features that are separated by occasional pits and coalescence boundaries. These step-flow features are characterized by arrays of curved terraces (as part of spiral growth hillocks) with step heights of $\sim 3 \text{ \AA}$ corresponding to the monolayer height of $c/2=2.88 \text{ \AA}$ for bulk InN. Increasing the growth temperature to 595 °C [Fig. 1(d)] resulted in much rougher surface (rms=18.7 nm). In this case, a higher density of metallic In droplets was observed on the surface (including small nuclei of droplets indicated by the arrows), as a result of increased In accumulation due to significant thermal dissociation of InN and limited In desorption at these temperatures.²² Note that the step-flow surface morphologies generated under In-

rich conditions are similar to those commonly observed for GaN growth under metal-rich conditions.¹⁷ Recent experiments have demonstrated that the GaN growth front is stabilized by a metallic Ga adlayer,²³ which promotes quite high N-adatom surface diffusion. Analogously, we have found an In adlayer on the N-face InN surface under In-rich conditions with a saturation coverage of 1 ML (as determined by In adsorption experiments using RHEED Bragg spot intensity variations).²² High-temperature InN growth under N-rich conditions, however, is remarkably different from what is known for GaN growth. As shown in Fig. 1(c), the terrace-like surface structure exhibits step-flow features, as also observed by Xu and Yoshikawa.¹⁵ These smooth surfaces indicate that high surface diffusion of In and N adatoms must be prevalent even in N-rich growth. We assume that the diffusion barrier for In adatoms on a bare InN surface is likely to be smaller than the barrier for Ga migration on a GaN surface.

To correlate the AFM surface morphologies with the structural quality, we have systematically determined the x-ray rocking curve (ω scans) widths [full width at half maximum (FWHM)] of on-axis and off-axis reflections (the latter measured in a skew-symmetric geometry) of several InN layers grown in the temperature range between 500 and 595 °C. For the more important off-axis scans we observe no dependence between FWHM values and growth conditions (both temperature and In/N flux ratio), with values scattered randomly between 1020 and 1200 arc sec for the $(10\bar{2}2)$ reflection and between 1320 and 1550 arc sec for the $(20\bar{2}1)$ reflection. These results indicate that the twist about the c axis is negligibly impacted by the growth conditions. In accordance with investigations of GaN by Heying *et al.*,²⁴ this means that the majority of pure edge-type threading dislocations (TDs) are essentially invariant with growth conditions. In contrast, we observe a slight dependence of the on-axis (0002) FWHM values [i.e., representing minority pure screw and mixed TDs (Ref. 24)] on the growth conditions, giving the lowest FWHM (~ 320 arc sec) for layers grown under In-rich conditions in a moderately low temperature range (500–540 °C). These values are comparable with the best values reported for N-face InN (Ref. 15) and are in general slightly better than those realized for In-face InN.^{14,25}

The significance of choosing optimum conditions of low growth temperature and In-rich conditions for the optical properties of N-face InN is illustrated in Fig. 2. Room-temperature PL, reflectance, and transmission data were obtained on optimized InN layers grown on N-face GaN buffer layers on C-face SiC substrates. The absorption coefficient was determined from both the reflectance and transmission data, and its square is plotted versus photon energy to determine the direct band gap of the InN. The intercept of the linear fit with the energy axis provides a band gap of 0.651 eV. The PL peak emission from a thick sample was determined using a Lorentzian fit to the data to occur at ~ 0.626 eV, with a FWHM of 54 meV. The slight redshift with respect to the band gap implies that the emission emanates primarily from the bandtail states. The band gap and PL peak emission energy are among the lowest reported values for wurtzite InN.^{1–3,14,15,26}

Finally, the transport properties were evaluated using an InN series with different thicknesses under identical and optimized conditions ($T=535$ °C, In/N=1.4) on a 200 nm

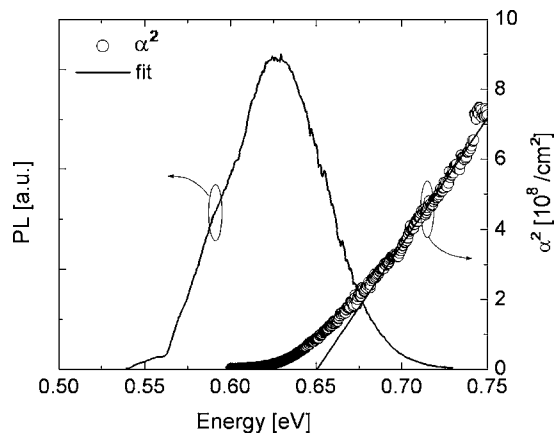


FIG. 2. Band gap obtained from absorption data and PL spectrum from optimized N-face InN samples.

thick N-face GaN buffer layer grown on semi-insulating C-face 6H-SiC substrates. To facilitate this we performed Hall measurements at 300 K on the as-grown InN layers (containing a small density of In droplets), with their results shown in Fig. 3. The Hall electron mobility increases continually with increasing layer thickness, reaching a maximum mobility of $2370 \text{ cm}^2/\text{V s}$ for a layer thickness of $4.4 \mu\text{m}$. These electron mobilities are almost a factor of 2 higher, and the corresponding bulk carrier concentration of $2.8 \times 10^{17} \text{ cm}^{-3}$ is nearly one order of magnitude lower than those reported for the best MBE grown N-face InN.¹⁵ By linear extrapolation of the sheet carrier concentration of the InN layers to zero thickness (for a series of samples grown to different InN thickness), a surface electron accumulation layer density of $\sim 3 \times 10^{13} \text{ cm}^{-2}$ was determined. The surface carrier concentration is in close agreement with the $\sim 2.5 \times 10^{13} \text{ cm}^{-2}$ density determined independently by energy electron loss spectroscopy and theoretical calculations.²⁷ Despite this consistency, we suggest that a more detailed analysis is needed for differentiating between bulk conduction and surface or interface conduction.

In summary, systematic growth kinetics studies were conducted to optimize the surface and structural properties of N-face InN grown on freestanding GaN. InN films with high

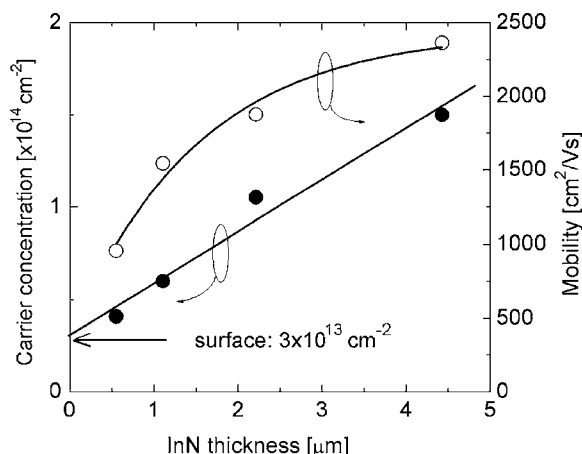


FIG. 3. Dependence of room-temperature Hall mobility and sheet carrier concentration on layer thickness for InN grown on N-face GaN on C-face 6H-SiC templates. A linear extrapolation of the carrier concentration to zero thickness yields an estimate of $\sim 3 \times 10^{13} \text{ cm}^{-2}$ for the surface electron density.

structural quality and smooth step-flow-like surface morphologies were achieved in a rather low-temperature region of $500\text{--}540 \text{ }^\circ\text{C}$ under In-rich conditions. The structural quality of InN was facilitated by the multiple effect of negligible thermal decomposition at these temperatures and the autosurfactant action of a 1 ML thick In adlayer on the surface. The band gap of 0.651 eV and room-temperature PL peak emission at 0.626 eV of our optimized InN are among the lowest reported values. In addition, Hall mobilities reached $2370 \text{ cm}^2/\text{V s}$ at bulk carrier concentrations in the low 10^{17} cm^{-3} , and a surface accumulation layer with an electron density of $\sim 3 \times 10^{13} \text{ cm}^{-2}$ was determined.

The authors gratefully acknowledge C. G. Van de Walle and D. Segev for many helpful discussions. This work was supported by DARPA (CNID program) and AFOSR (D. J. Silversmith, program manager).

¹V. Yu. Davydov, A. A. Klochikhin, R. P. Seisyan, V. V. Emtsev, S. V. Ivanov, F. Bechstedt, J. Furthmüller, H. Harima, A. V. Mudryi, J. Aderhold, O. Semchinova, and J. Graul, *Phys. Status Solidi B* **229**, R1 (2002).

²J. Wu, W. Walukiewicz, K. M. Yu, J. W. Ager, E. E. Haller, H. Lu, W. J. Schaff, Y. Saito, and Y. Nanishi, *Appl. Phys. Lett.* **80**, 3967 (2002).

³T. Matsuoka, H. Okamoto, M. Nakao, H. Harima, and E. Kurimoto, *Appl. Phys. Lett.* **81**, 1246 (2002).

⁴R. Ascazubi, I. Wilke, K. Denniston, H. Lu, and W. J. Schaff, *Appl. Phys. Lett.* **84**, 4810 (2004).

⁵M. Higashiwaki and T. Matsui, *Jpn. J. Appl. Phys., Part 2* **41**, L540 (2002).

⁶V. M. Polyakov and F. Schwierz, *Appl. Phys. Lett.* **88**, 032101 (2006).

⁷S. K. O'Leary, B. E. Foutz, M. S. Shur, and L. F. Eastman, *Appl. Phys. Lett.* **87**, 222103 (2005).

⁸J. Wu, W. Walukiewicz, W. Shan, K. M. Yu, J. W. Ager, S. X. Li, E. E. Haller, H. Lu, and W. J. Schaff, *J. Appl. Phys.* **94**, 4457 (2003).

⁹C. S. Gallinat, G. Koblmüller, S. Bernardis, J. S. Brown, J. S. Speck, G. D. Chern, E. D. Readinger, H. Shen, and M. Wraback, *Appl. Phys. Lett.* **89**, 032109 (2006).

¹⁰H. Lu, W. J. Schaff, J. Hwang, H. Wu, G. Koley, and L. F. Eastman, *Appl. Phys. Lett.* **79**, 1489 (2001).

¹¹Y. Saito, N. Teraguchi, A. Suzuki, T. Araki, and Y. Nanishi, *Jpn. J. Appl. Phys., Part 2* **40**, L91 (2001).

¹²C. J. Lu, L. A. Bendersky, H. Lu, and W. J. Schaff, *Appl. Phys. Lett.* **83**, 2817 (2003).

¹³E. Dimakis, E. Iliopoulos, K. Tzagaraki, and A. Georgakilas, *Appl. Phys. Lett.* **86**, 133104 (2005).

¹⁴T. Iwe, O. Brandt, M. Ramsteiner, M. Gehler, H. Kostial, and K. H. Ploog, *Appl. Phys. Lett.* **84**, 1671 (2004).

¹⁵K. Xu and A. Yoshikawa, *Appl. Phys. Lett.* **83**, 251 (2003).

¹⁶H. Naoi, F. Matsuda, T. Araki, A. Suzuki, and Y. Nanishi, *J. Cryst. Growth* **269**, 155 (2004).

¹⁷B. Heying, R. Averbeck, L. F. Chen, E. Haus, H. Riechert, and J. S. Speck, *J. Appl. Phys.* **88**, 1855 (2000).

¹⁸G. Koblmüller, R. Averbeck, L. Geelhaar, H. Riechert, W. Hoesler, and P. Pongratz, *J. Appl. Phys.* **93**, 9591 (2003).

¹⁹S. Rajan, M. Wong, Y. Fu, F. Wu, J. S. Speck, and U. K. Mishra, *Jpn. J. Appl. Phys., Part 2* **44**, L1478 (2005).

²⁰E. Monroy, E. Sarigiannidou, F. Fossard, N. Gogneau, E. Bellet-Amalric, J.-L. Rouviere, S. Monnoye, H. Mank, and B. Daudin, *Appl. Phys. Lett.* **84**, 3684 (2004).

²¹A. R. Smith, R. M. Feenstra, D. W. Greve, M. S. Shin, M. Skowronski, J. Neugebauer, and J. E. Northrup, *Appl. Phys. Lett.* **72**, 2114 (1998).

²²G. Koblmüller, C. S. Gallinat, and J. S. Speck (unpublished).

²³G. Koblmüller, R. Averbeck, H. Riechert, and P. Pongratz, *Phys. Rev. B* **69**, 035325 (2004).

²⁴B. Heying, X. H. Wu, S. Keller, Y. Li, D. Kopolnek, B. P. Keller, S. P. DenBaars, and J. S. Speck, *Appl. Phys. Lett.* **68**, 643 (1996).

²⁵V. V. Mamutin, V. A. Vekshin, V. Y. Davydov, V. V. Ratnikov, T. V. Shubina, S. V. Ivanov, P. S. Kopev, M. Karlsteen, U. Södervall, and M. Willander, *Phys. Status Solidi A* **176**, 247 (1999).

²⁶M. Higashiwaki and T. Matsui, *J. Cryst. Growth* **269**, 162 (2004).

²⁷I. Mahboob, T. D. Veal, C. F. McConville, H. Lu, and W. J. Schaff, *Phys. Rev. Lett.* **92**, 036804 (2004).